Regular Article

THROMBOSIS AND HEMOSTASIS

Brain-derived microparticles induce systemic coagulation in a murine model of traumatic brain injury

Ye Tian,[1,2] Breia Salsbery,[2] Min Wang,[3] Hengjie Yuan,[1,2] Jing Yang,[2] Zilong Zhao,[1] Xiaoping Wu,[2] Yanjun Zhang,[1] Barbara A. Konkle,[2,4] Perumal Thiagarajan,[5,6] Min Li,[3] Jianning Zhang,[1] and Jing-fei Dong[2,4]

[1]Tianjin Neurological Institute, Department of Neurosurgery, General Hospital, Tianjin Medical University, Tianjin, China; [2]Puget Sound Blood Research Institute, Seattle, WA; [3]Institute of Pathology, School of Basic Medical Sciences, Lanzhou University, Lanzhou, China; [4]Division of Hematology, Department of Medicine, University of Washington School of Medicine, Seattle, WA; [5]Departments of Pathology and Medicine, Baylor College of Medicine, Houston, TX; and [6]Center for Translational Research on Inflammatory Diseases, Michael E. DeBakey VA Medical Center, Houston, TX

Key Points

- Brain-derived cellular microparticles induce systemic coagulopathy in traumatic brain injury.
- Platelets facilitate the transmigration of brain microparticles through the endothelial barrier into the circulation.

Traumatic brain injury (TBI) is associated with coagulopathy, although it often lacks 2 key risk factors: severe bleeding and significant fluid resuscitation associated with hemorrhagic shock. The pathogenesis of TBI-associated coagulopathy remains poorly understood. We tested the hypothesis that brain-derived microparticles (BDMPs) released from an injured brain induce a hypercoagulable state that rapidly turns into consumptive coagulopathy. Here, we report that mice subjected to fluid percussion injury (1.9 ± 0.1 atm) developed a BDMP-dependent hypercoagulable state, with peak levels of plasma glial cell and neuronal BDMPs reaching 17 496 ± 4833/μL and 18 388 ± 3657/μL 3 hours after TBI, respectively. Uninjured mice injected with BDMPs developed a dose-dependent hyper-turned hypocoagulable state measured by a progressively prolonged clotting time, fibrinogen depletion, and microvascular fibrin deposition in multiple organs. The BDMPs were 50 to 300 nm with intact membranes, expressing neuronal or glial cell markers and procoagulant phosphatidylserine and tissue factor. Their procoagulant activity was greater than platelet microparticles and was dose-dependently blocked by lactadherin. Microparticles were produced from injured hippocampal cells, transmigrated through the disrupted endothelial barrier in a platelet-dependent manner, and activated platelets. These data define a novel mechanism of TBI-associated coagulopathy in mice, identify early predictive markers, and provide alternative therapeutic targets. (*Blood*. 2015;125(13):2151-2159)

Introduction

Uncontrolled hemorrhage is a leading cause of the preventable deaths that occur in patients with trauma, accounting for 30% to 40% of all trauma fatalities.[1,2] It is caused by direct injury to the vasculature and a resulting secondary coagulopathy. The causes of trauma-associated coagulopathy include blood loss, consumption of coagulation factors and platelets, the dilution of coagulation factors and platelets due to fluid resuscitation, and hypothermia.[3,4] Recent studies also implicate a role of activated protein C in the coagulopathy associated with severe trauma.[5,6]

Retrospective and observational studies have consistently shown that coagulopathy is common in patients with traumatic brain injury (TBI).[7-11] However, isolated TBI lacks 2 key causal factors for coagulopathy associated with injury to the trunk and limbs, heavy blood loss and a large volume of fluid resuscitation, suggesting that it follows a distinct pathogenic pathway. The finding that coagulopathy is common in patients with penetrating brain injury[10] further indicates that damage to cerebral tissue plays a role in developing the coagulopathy. In a study of 972 TBI patients with coagulopathy,

D-dimer and fibrinogen degradation products were detected minutes after injury, followed by a profound depletion of fibrinogen.[8] Prolonged prothrombin and partial thromboplastin times usually occurred late, indicating a transition from a hyper- to a hypocoagulable state.[8,9]

Despite strong clinical and laboratory evidence of its presence and association with poor clinical outcomes,[12] the pathogenesis of TBI-associated coagulopathy remains poorly understood. Current clinical tests detect the coagulopathy, but are insufficient to determine its causes or to predict its occurrence, making clinical management of TBI-associated coagulopathy difficult and costly. We hypothesized that brain-derived procoagulant molecules delivered in the form of cellular microparticles play a role in developing systemic coagulopathy after TBI. This hypothesis is derived from several observations. First, the brain is enriched in procoagulant anionic phospholipids, such as phosphatidylserine (PS), which provide a negatively charged surface to initiate and propagate coagulation.[13] These anionic phospholipids are normally present on the inner

---

leaflet,[14] whereas neutral phospholipids, such as phosphatidylcholine (PC) and sphingomyelin, are on the external leaflet of the cell membrane.[15] This asymmetry is lost in cells subjected to traumatic and/or ischemic injuries, exposing PS on the outer membrane.[16] Second, tissue factor (TF), which initiates the extrinsic pathway of coagulation on platelets, is also richly expressed on neurons and glial cells.[17-19] A long-standing question is how TF and PS are integrated into the membrane of activated platelets, which express no or an extremely low level of TF,[20,21] to initiate the coagulation during trauma hemostasis. One potential mediator is cellular microparticles.

Microparticles are cell fragments produced from activated or apoptotic cells.[22,23] They are primarily composed of the plasma membrane along with a limited amount of cytoplasm and measure 0.1 to 1 μm in diameter.[23] They are enriched in the lipid microdomains, where cholesterol, phospholipids, and receptors are clustered.[24,25] These microparticles promote coagulation by providing PS-dependent binding sites for the assembly of a prothrombinase and tenase complex[26] and by adhering to or fusing with the platelet membrane.[27] Although microparticles from blood cells have been detected at high levels in TBI patients,[28,29] those released from an injured brain have not been studied. Neural cells are highly sensitive to mechanical and ischemic injuries, potentially leading to microvesiculation.[30-32] However, it is not known whether (1) an injury induces neural cells to vesiculate, (2) brain-derived microparticles (BDMPs) are released into the systemic circulation, or (3) BDMPs induce intravascular coagulation. Here, we report that highly procoagulant BDMPs are detected in the systemic circulation and induce coagulation in mice either subjected to TBI or infused with BDMPs.

Materials and methods

Mouse model of fluid percussion injury

Adult male C57BL/6J mice (12-16 weeks old and 22-25 g; Jackson Laboratory, Bar Harbor, ME) were subjected to fluid percussion injury (FPI).[33] Briefly, a mouse was anesthetized by ketamine and xylazine (1 mg and 0.1 mg/10 g) on a ventilator (Harvard Apparatus, Hollistone, MA) and constrained to a platform to surgically expose the skull. A 3-mm-diameter hole was drilled into the skull (2.0-mm posterior from the bregma and 2.0-mm lateral to the sagittal suture) with the dura matter intact. A female Leur-Lok was cemented to the craniotomy site of the mouse that had been allowed to recover from the surgery for 60 minutes and was connected to an FPI device (Custom Design & Fabrication, Richmond, VA). With the head unrestrained, saline from a Plexiglas cylindrical reservoir was rapidly injected into the closed cranial cavity at a controlled pressure of 1.9 ± 0.1 atm. A sham mouse underwent the same surgery without being exposed to FPI. To model the acute events and to minimize impacts of secondary injury, all mice were examined within the first 6 hours after FPI. The mouse study is approved by the Institutional Animal Care and Use Committees of the Puget Sound Blood Center.

Detection of brain-derived microparticles

Neuron- and glial cell-derived microparticles (collectively termed BDMPs) were identified by a modified flow cytometry-based method (supplemental Figure 1, available on the *Blood* Web site).[34] They were first identified by their size (<1 μm) using standard microbeads that were 0.5, 0.9, and 3 μm in diameter (Biocytex, Marseille, France) and then by their expression of neuron-specific enolase (NSE) and glial fibrillary acidic protein (GFAP) using fluorescein isothiocyanate-conjugated monoclonal (Abcam, Cambridge, MA)

and polyclonal antibodies (eBioscience, San Diego, CA) on an LSR II flow cytometer (Beckon Dickinson, San Jose, CA) (supplemental Figure 8). Isotype-specific immunoglobulin (Ig)Gs and a rabbit nonimmune IgG were used as negative controls. To reduce small particle contaminants, buffers were filtered with a 0.1-μm filter (EDM Millipore, Billerica, MA) before use. The data were presented as the percent of Annexin V$^+$ and neural marker$^+$ microparticles in the microparticle gate set by microbeads unless otherwise specified. To validate the data and address the concern that NSE is also expressed in platelets and erythrocytes,[35,36] BDMPs were also probed with monoclonal antibodies against the neuronal marker Na$^+$/K$^+$ ATPase α3 and the glial marker glutamate transporter 1 (both from EMD Millipore).

The expression of TF and PS on BDMPs was detected using a phycoerythrin (PE)-conjugated polyclonal antibody (Bioss, Woburn, MA) and allophycocyanin (APC)-conjugated Annexin V (eBioscience), respectively. EDTA (5 mM) was used to test the specificity of this assay (supplemental Figure 2). BDMPs were quantified by double-labeling with antibodies to GFAP/NSE and annexin V binding.

Coagulation assays

Two coagulation assays were performed to evaluate BDMP-associated procoagulant activity to assess relative contributions of PS and TF. The first was a PS-dependent assay that tested the ability of BDMPs to promote clot formation in the presence of coagulation factor Xa.[37] For each reaction, 25 μL of phosphate-buffered saline (PBS) containing a known number of BDMPs was mixed with 25 μL of phospholipid-deficient porcine plasma (IMVS, Adelaide, Australia) and 100 μL of bovine factor Xa (0.02 U/mL in a buffer containing 15 mM CaCl$_2$, 100 mM NaCl, 20 mM N-2-hydroxyethylpiperazine-N'-2-ethanesulfonic acid, and 0.001% polybrene [pH 7.0]). Clot formation was monitored at 37°C on a CoaScreener coagulation analyzer (American Labor Corp., Durham, NC). Purified brain PS and PC (Avanti Polar Lipids, Alabaster, AL) were used as positive and negative controls, respectively. The calcium dependence of this assay was determined by treating samples with 4 mM of EDTA (supplemental Figure 3). For mouse experiments, blood collected after injury or infused with BDMPs was centrifuged at 1500g for 20 minutes at 25°C to collect platelet-poor plasma (PPP). PPP was either tested directly or processed to generate microparticle-free plasma (MPFP). To obtain MPFP, PPP was centrifuged at 13 000g for 2 minutes at room temperature to obtain the cell-free supernatant, which was centrifuged twice at 100 000g (4°C, 60 minutes) to remove microparticles. The second assay measured the ability of BDMP-bound TF to promote thrombin generation in the presence of phospholipids using a commercial kit (supplemental Methods).[38]

Binding of lactadherin to BDMPs

FITC-conjugated bovine lactadherin (Haematologic Technologies, Essex Junction, VT) was incubated with purified BDMPs for 30 minutes and then with a PE-conjugated monoclonal glutamate transporter 1 antibody (EMD Millipore) for 20 minutes. Lactadherin binding was detected by FITC fluorescence on glutamate transporter 1$^+$ BDMPs in the absence and presence of an ~100-fold excess unlabeled lactadherin (Haematologic Technologies) or increasing concentrations of brain PS and PC.

Culture of neural cells and microparticle production

Hippocampi were dissected from sacrificed newborn C57BL/6J mice and washed with PBS. They were incubated for 20 minutes at 37°C with Hibernate A medium containing 2% B27 serum-free supplement (Life Technologies, Grand Island, NY), 0.5 mM L-glutamine (Life Technologies), and 2 mg/mL papain (Worthington Biochemical Corp., Lakewood, NJ). Partially digested hippocampi were incubated with 0.2 mg/mL DNAse I for 5 minutes at 37°C and dispersed into a homogenous cell suspension. After viability measured using a Trypan blue exclusion test, 2 to 4 × 10^5 viable cells were plated on a 35-mm culture dish coated with 50 μg/mL of poly-D-lysine (Sigma-Aldrich, St. Louis, MO) and cultured in Neurobasal-A medium (2% B27 serum-free supplement, 0.5 mM L-glutamine, and 5 ng/mL

basic fibroblast growth factor; Life Technologies) at 37°C. After 7 days in culture, cells were washed with PBS and stimulated with 15 µM of the calcium ionophore A23187 (Fisher Bioreagents, Waltham, MA), which served as a surrogate for cell injury, for 30 minutes at 37°C. Media from the stimulated and unstimulated cells were collected and centrifuged at 16 000g for 10 minutes. Microparticles in the supernatant were detected by flow cytometry.

BDMP transmigration through the endothelial cell barrier

PKH26 (Sigma-Aldrich) has a long aliphatic tail that stably incorporates into lipid regions of the cell membrane, emitting yellow-orange fluorescence.[39] BDMPs were incubated with 5 µM PKH26 for 5 minutes at room temperature. The labeling was stopped by the addition of 500 µL of 10% bovine serum albumin (1 minute at room temperature). PKH26-labeled BDMPs were collected by centrifugation at 100 000g for 1 hour at 4°C and resuspended in PBS for immediate experiments.

For transmigration experiments, human umbilical vein endothelial cells (HUVECs; Lonza, Basel, Switzerland) were grown in Endothelial Growth Basal Medium (Lonza) on a collagen-coated polytetrafluoroethylene membrane (0.4-µm pore) that forms the base of a transwell (Corning, Tewksbury, MA). Confluent HUVECs were stimulated with 25 µM of histamine for 20 minutes at 37°C. After washing, PKH26-labeled BDMPs at 1×10^7/mL were incubated with resting and activated HUVECs in the presence and absence of live or lyophilized platelets (300 000/µL) for 3 hours at 37°C. The medium in the bottom chamber was collected and analyzed for BDMPs by flow cytometry (supplemental Figure 4).

Effects of BDMPs on platelets

Human blood samples were collected in 0.38% sodium citrate from healthy subjects under an approved institutional review board protocol. They were centrifuged at 150g for 15 minutes at 25°C to collect platelet-rich plasma (PRP). Platelet counts were normalized to 2.5×10^5/µL using homologous plasma. Platelet aggregation induced by 1×10^4/µL of BDMPs, in the presence and absence of type I collagen (Helena Laboratories, Beaumont, TX), was monitored at 37°C for 10 minutes in an AggRAM optical aggregometer (Helena Laboratories). To measure CD62p and PS expression, platelets were incubated with 1×10^4/µL BDMPs in the presence of either a PE-conjugated CD62p antibody (BD Biosciences, San Jose, CA) or APC labeled-annexin V for 30 minutes at 37°C. The calcium influx in platelets induced by BDMPs was measured using a commercial probe (supplemental Methods).

To measure the BDMP interaction with platelets, PKH26-labeled BDMPs were incubated at 37°C with PRP and an FITC-conjugated antibody against the platelet-specific marker CD42b (BD Biosciences) for 30 and 20 minutes, respectively. Platelets (CD42b⁺) were analyzed for PKH26 fluorescence at 567 nm by flow cytometry.

Electron microscopy

Purified BDMPs were first fixed in 2.5% glutaraldehyde for 24 hours at 4°C, followed by washing with PBS and fixation in 1% osmium tetroxide for 1.5 hours at 4°C. They were dehydrated in solutions with increasing concentrations of ethanol and embedded in Epon 812. Ultrathin sections were made and sequentially treated with uranyl acetate and lead citrate before they were dried by heat. The slides were observed under transmission electron microscopy (TEM; JEM-1230). For an enhanced view of the plasma membrane, BDMPs loaded onto carbon-coated formvar grids for 1 minute were stained with phosphotungstic acid (pH 6.8) for 2 minutes.[40,41] To specifically identify BDMPs, a colloid gold-conjugated goat anti-rabbit antibody was immobilized onto the grids for 20 minutes. These coated grids were washed and incubated with BDMPs that had been pre-incubated with a rabbit anti-GFAP antibody (ZSGB-Bio; 4°C overnight) for 4 hours before being processed for TEM. Scanning electron microscopy was also used to observe the BDMP-platelet interaction (supplemental Methods).[42]

Statistical analysis

Categorical (frequency) variables were expressed as percentages and continuous variables as the mean ± standard error of the mean. Data were analyzed using Sigma plot (V. 11.2) for the paired t test or 1-way or repeated-measures analysis of variance (ANOVA) as specified in each dataset. $P < .05$ was considered statistically significant.

Results

Development of a BDMP-dependent hypercoagulable state in TBI mice

At a mean fluid pressure of 1.9 ± 0.1 atm generated from an FPI device, mice sustained cerebral injury visible at the site of impact (Figure 1A). When measured by a PS-dependent clotting assay, plasma from TBI mice had a significantly shortened (accelerated) clotting time compared with plasma from mice with sham surgery (Figure 1B). This shortened clotting time was reversed when microparticles were removed from the plasma (Figure 1C). In parallel with changes in the clotting time, glial cell-(GFAP⁺) and neuron-derived (NSE⁺) BDMPs were detected in blood samples from the TBI mice (Figure 1D-E), but not in mice before being subjected to either FPI or sham surgery (the baseline levels for noninjured mice and IgG isotype controls were at $0.025 \pm 0.019\%$ and $0.038 \pm 0.016\%$, respectively). The presence of these BDMPs was further verified by a second set of neuronal (Na⁺/K⁺ ATPase α3) and glial cell (glutamate transporter 1) markers (supplemental Figure 5). BDMPs reached peak levels 3 hours after injury (Figure 1D-E), with mean levels at 17 496 ± 4833/µL and 18 388 ± 3657/µL of GFAP⁺ and NSE⁺ microparticles, respectively. The numbers of BDMPs at other time points were calculated by extrapolating values at peak levels 3 hours after TBI (supplemental Figure 6) and found to be consistent. The level of plasma GFAP⁺ microparticles decreased 6 hours after injury, whereas NSE⁺ microparticles remained relatively constant. A portion of these BDMPs expressed PS as detected by annexin V (Figure 1F). The percentage of PS⁺ BDMPs varied considerably among individual mice, accounting for 39 ± 21% and 42 ± 26% of total GFAP⁺ and NSE⁺ microparticles, respectively.

BDMPs were also detected in blood samples from mice that had undergone sham surgery (Figure 1D-E), but reaching peak levels of 1853 ± 745/µL (GFAP⁺) and 2153 ± 889/µL (NSE⁺), significantly lower than those found in TBI mice (n = 12, $P < .01$).

Procoagulant activity of BDMPs

Specifically investigating the role of BDMPs in the development of TBI-associated coagulopathy is challenging in mice with FPI, because microparticles from endothelial and blood cells are also released in response to traumatic stress. To overcome this technical challenge, we generated BDMPs from the brains of adult C57BL/6J mice by freeze-thawing injury.[37] The BDMPs thus produced resemble those detected in the plasma of FPI mice in size and levels of PS and GFAP expression (supplemental Figure 7). When viewed under TEM, these BDMPs were irregular spheres of 50 to 500 nm in diameter, with a clearly defined and relatively intact membrane, but without apparent granules (Figure 2A). They expressed NSE and GFAP (Figure 2B) and could be classified as TF⁺, PS⁺, and TF⁺/PS⁺ microparticles (Figure 2C). In contrast, we did not detect von Willebrand factor (Figure 2B), a common marker for Weibel-Palade
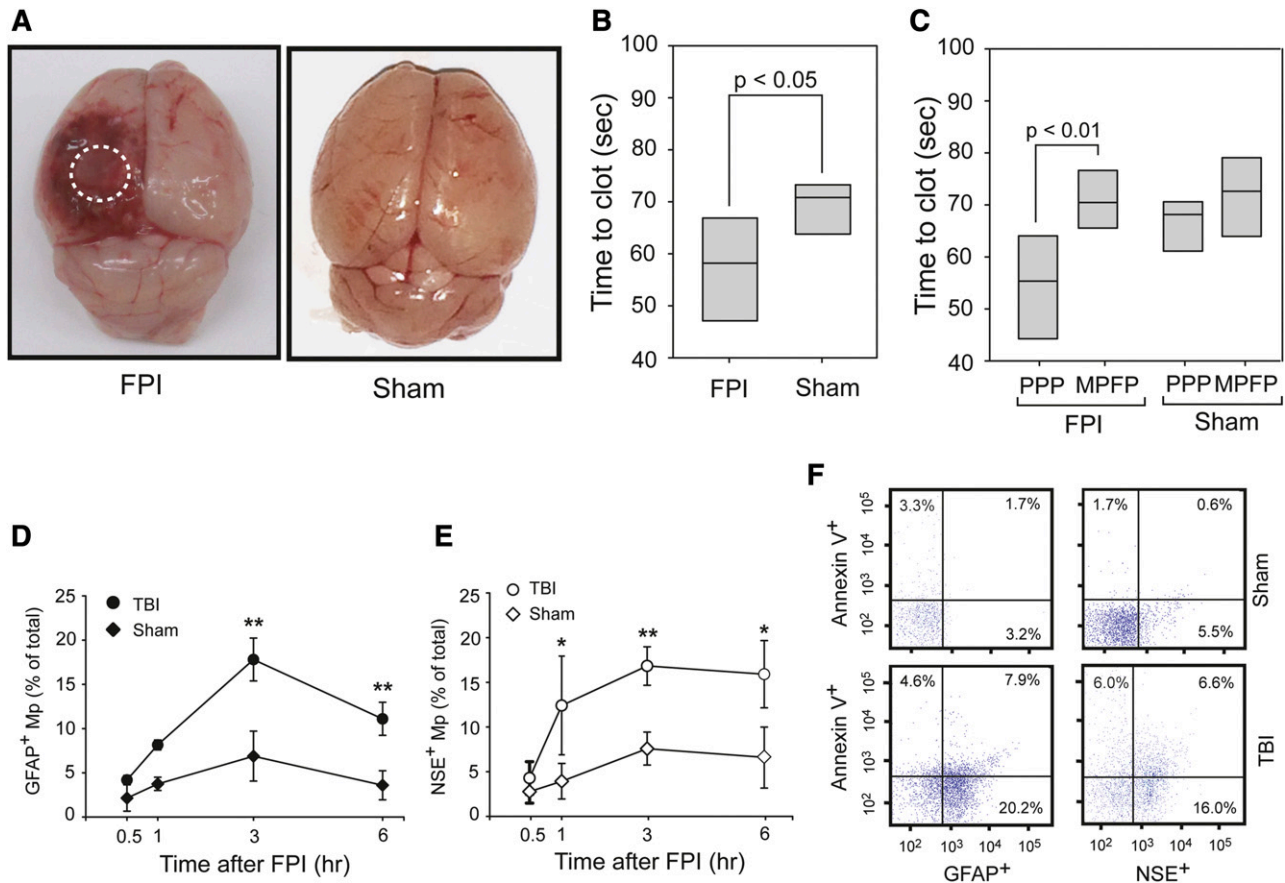
Figure 1. FPI-induced and BDMP-dependent coagulation. (A) Cerebral injury is visible in the left parietal lobe of a mouse 3 hours after FPI compared with the brain from a mouse subjected to sham surgery. (B) The clotting time of PPP collected from mice 3 hours after FPI or sham surgery was measured in a PS-dependent assay (n = 6, paired t test). (C) Clotting times were compared between PPP and homologous MPFP collected from mice subjected to FPI and sham surgery (n = 9, paired t test). (D-E) GFAP$^+$ and NSE$^+$ microparticles were detected by flow cytometry over time in blood samples from TBI and sham mice (n = 6 at each time point), and the values are after the subtraction of values from isotype IgGs (1-way ANOVA, n = 48, *$P < .01$, **$P < .05$). (F) Fractions of GFAP$^+$ and NSE$^+$ microparticles that express PS as measured by annexin V binding (a representative of 16 separate experiments).

bodies of endothelial cells and α-granules of platelets that overlap in size (~50-200 nm) and could be copurified along with BDMPs. The surface markers for leukocytes (CD45), endothelial cells (CD144), and erythrocytes (CD235a) were also negative (supplemental Figure 8), suggesting that the contaminants from blood and endothelial cells were below the detection in these BDMP preparations.

When added to phospholipid-free plasma, BDMPs accelerated the rate of PS-dependent clot formation in a dose-dependent manner, reaching a maximal activity at ~1×10^5 BDMPs/μL, which was equivalent to 1.6 μg/μL of purified brain PS (Figure 2D). This PS-dependent procoagulant activity was blocked by the PS-binding protein lactadherin (Figure 2E), which bound BDMPs (supplemental Figure 9). The BDMP-lactadherin interaction was partially blocked by purified PS but not PC (supplemental Figure 10). In comparable numbers, BDMPs were significantly more active in promoting clot formation than the microparticles generated from platelets activated by collagen, which is known to induce platelet microvesiculation (supplemental Methods; supplemental Figure 11).[43] These platelet microparticles expressed PS, but not TF at a detectable level (supplemental Figure 12). BDMPs also promoted thrombin generation in a TF-dependent assay, where 25 000/μL of BDMPs had an activity equivalent to 1 pM of soluble TF (Figure 2E). This BDMP-induced thrombin generation had a significantly delayed

onset and a smaller area under the curve (AUC; Table 1). In both assays, the number of BDMPs that induced a maximal level of coagulation (Figure 2D-E) was comparable to that detected in FPI mice (Figure 1D-E).

To specifically measure the procoagulant activity of BDMPs in vivo, we injected BDMPs into uninjured mice through the tail vein and collected blood samples 30 minutes after injection to measure the rate of clot formation and the level of plasma fibrinogen. The lungs, kidney, and heart were also collected at the same time and evaluated for fibrin deposition, a hallmark of consumptive coagulopathy. In this experimental setting, mice injected with 1×10^4/μL of BDMPs showed a tendency toward a shortened clotting time. Further increases in the number of BDMPs resulted in a progressively prolonged clotting time (Figure 3A). Consistent with this dose-dependent biphasic hyper-turned hypocoagulable state, the plasma level of fibrinogen was progressively reduced by an increasing number of BDMPs injected (Figure 3B). Phosphotungstic acid hematoxylin stain revealed a widespread fibrin deposition in the microvasculature of the lungs, kidney, and heart of the mice injected with BDMPs, but not in the same organs of mice injected with PBS (Figure 3C-H). These data show that BDMPs induced a dose-dependent transition from a hypercoagulable state to consumptive coagulopathy, consistent with the phenotype observed in TBI mice and patients with TBI.
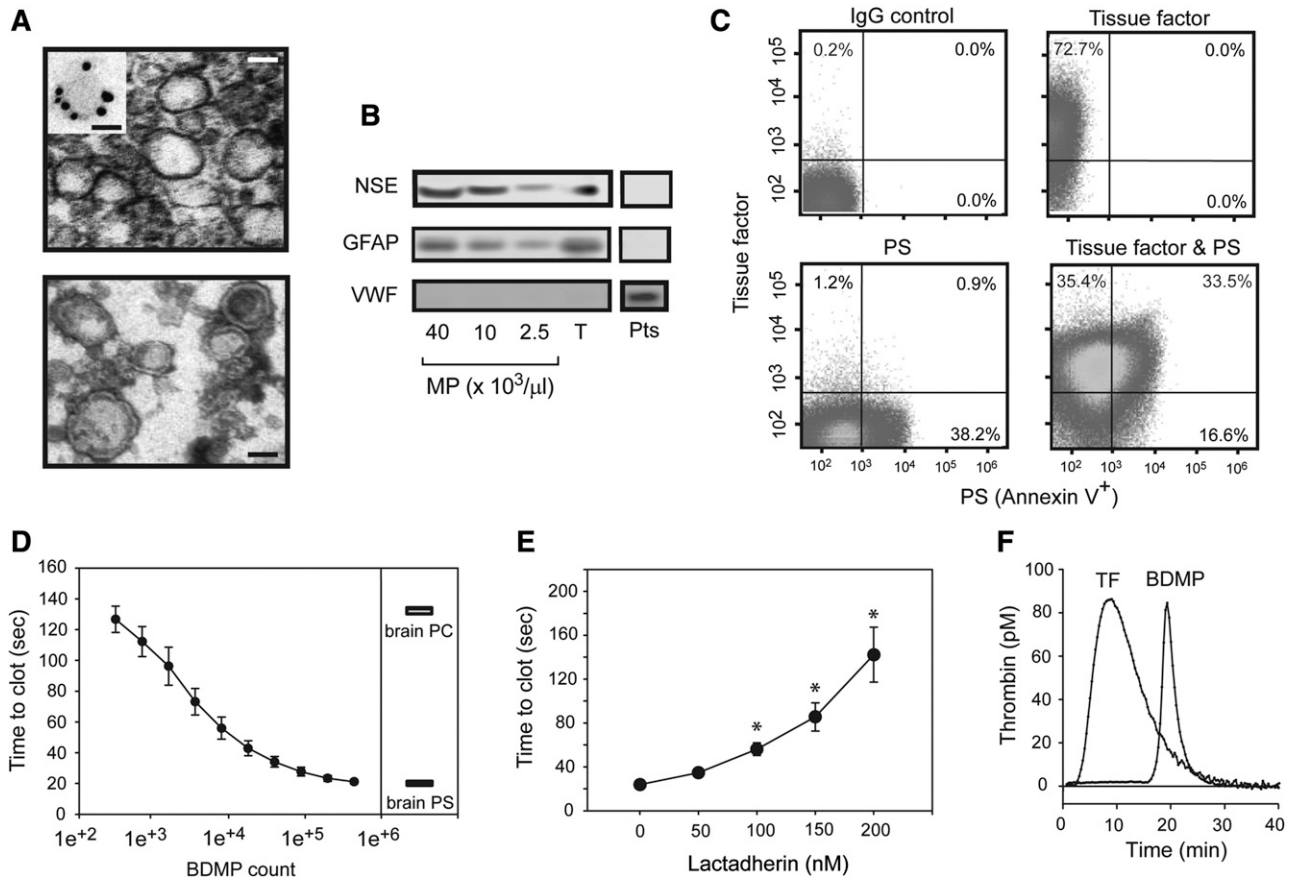
Figure 2. Procoagulant activity of BDMPs from freeze-thawing injury. (A) (Upper) TEM image of BDMPs (bar = 200 nm). (Inset) A microparticle stained with an immune-gold-labeled GFAP antibody (bar = 100 nm). (Lower) TEM image of BDMPs with negative staining to enhance the view of membrane structures (bar = 200 nm). (B) BDMPs and platelet microparticles solubilized in an SDS lysis buffer were probed for NSE, GFAP, and von Willebrand factor (T, whole brain lysate; Pts, platelet lysate as control). (C) The expression of TF, PS, and both was measured for BDMPs (represents 20 separate measurements). (D) PS-dependent clotting time was measured in the presence of increasing numbers of BDMPs (n = 6, 1-way ANOVA, $P < .001$) and compared with those induced by 1.6 μg/μL of purified brain PS and PC, respectively. (E) Plasma clotting times induced by 25 000/μL BDMPs were measured in the presence of increasing concentrations of bovine lactadherin. (F) TF-dependent thrombin generation was measured in reaction containing either 1 pM TF or 25 000 BDMPs (representative of 3 separate experiments).

BDMP production by injured brain cells and transmigration through the disrupted endothelial barrier

The data have thus far shown that the injured brain released BDMPs into the systemic circulation through the traumatized blood-brain barrier, resulting in intravascular coagulation. The extravasation of Evans blue was indeed observed in brains dissected from mice with FPI, but not from those with sham surgery (Figure 4A). The production and transmigration of BDMPs were further examined in vitro. Cultured hippocampal cells (Figure 4B) released microparticles after stimulation with the calcium ionophore A23187 (Figure 4C), an agent known to induce apoptosis and microvesiculation.[44] The ability of BDMPs to pass through the endothelial barrier was measured in a transwell system, where confluent HUVECs cultured in

the top chamber were first activated by histamine (Figure 4D), which increases vascular permeability by inducing endothelial cells to contract.[45,46] BDMPs were then loaded onto the endothelial cells in the presence or absence of live or lyophilized platelets. After incubation for 3 hours at 37°C, the time when the highest level of BDMPs was found in the blood of FPI mice (Figure 1), BDMPs were detected in the bottom chamber when they were incubated with histamine-stimulated HUVECs and live, but not lyophilized, platelets (Figure 4E). Live platelets also facilitated a lower rate of BDMP transmigration through unstimulated HUVECs. To further examine a role of platelets in promoting BDMP transmigrantion, we tested serotonin, a major component of platelet dense granules that is released on platelet activation[47] and is known to enhance the pro-coagulant properties of platelets[48] and to increase vascular permeability.[49] As shown in Figure 4E, serotonin at 5 μM promoted the transmigration of BDMPs through the endothelial barrier at a level similar to that induced by live platelets on histamine-stimulated HUVECs.

A role of platelets in assisting the transmigration of BDMPs through activated HUVECs was further examined by scanning electron microscopy that detected BDMPs on the transwell membrane in the opposite side of histamine-activated HUVECs incubated with BDMPs with, but not without, platelets (Figure 4F).

Table 1. Thrombin generation induced by BDMPs

Measure	TF (1 pM)	BDMP (2.5 × 10⁴/μL)	P value*
Lag time (min)	4.6 (0.9)	13.0 (2.6)	<.001
Peak concentration (nM)	89.3 (55.9)	90.8 (7.7)	.23
AUC (nM/min)	1196.4 (229.2)	300.0 (10.2)	<.001

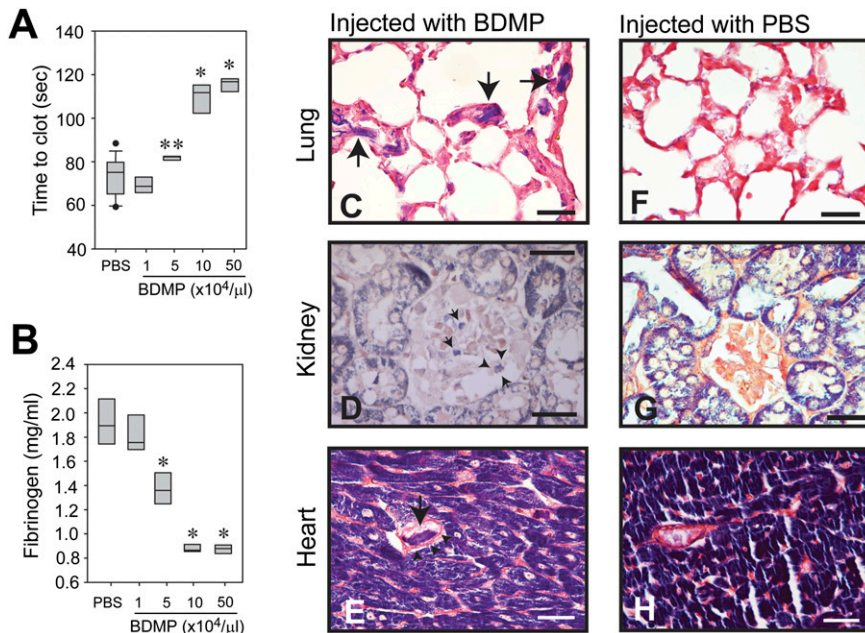Values are expressed as mean (standard deviation).
*Paired t test.

Figure 3. Coagulopathy induced by infusion of BDMPs into uninjured mice. (A) Blood samples were collected from mice infused with BDMPs or PBS and tested for PS-dependent clot formation (n = 12, 1-way ANOVA, **P = .036, *P < .001 compared with PBS). (B) Levels of fibrinogen were measured in the plasma samples collected for studies in A (n = 12, 1-way ANOVA, *P < .001 compared with PBS). Sections of formaldehyde-fixed lungs, kidney, and heart from mice injected with (C-E) BDMPs or (F-H) PBS were stained with phosphotungstic acid hematoxylin (dark blue; the dye also stains muscle cells). The left panel shows fibrin deposition in the microvasculature of the (C) lung, (D) kidney, and (E) stromatic vessels of the heart from mice injected with BDMPs (arrows). Arrowheads indicate intact walls of fibrin deposited vessels (bar = 25 μm). (F-H) Fibrin deposition was not detected in organs collected from mice receiving PBS (bar = 25 μm). Images are representative of 6 mice injected with BDMPs and 5 with PBS.

Effects of BDMPs on platelets

The data presented in Figure 4E-F suggest that platelets assisted the transmigration of BDMP through a disrupted endothelial barrier. Therefore, we examined whether this platelet-BDMP interaction affected platelet function. BDMPs were detected binding platelets by flow cytometry (Figure 5A) and scanning electron microscopy (Figure 5B). Furthermore, BDMPs induced rapid and time-dependent calcium influx in platelets that reached a plateau 15 minutes after the stimulation (Figure 5C). Platelets incubated with BDMPs also expressed CD62p (Figure 5D) and PS (Figure 5E). In contrast, BDMPs did not directly induce platelet aggregation or enhance collagen-induced platelet aggregation (Figure 5F).

Discussion

Acute changes in coagulation associated with TBI were studied using a mouse FPI model combined with reciprocal mouse and complementary in vitro experiments to identify their causes. We focused on the early hours after TBI (≤6 hours) to minimize confounding changes induced by secondary events, such as ischemic injury. We made several novel observations that define a causal role for BDMPs in the systemic coagulation associated with TBI in mouse models.

First, mice subjected to FPI developed a hypercoagulable state within 3 hours of the injury, and this hypercoagulable state was reversed when microparticles were removed (Figure 1). The development of this hypercoagulable state was associated in time with BDMPs reaching peak levels in the circulation. Although widely used as a neuronal marker, NSE is also detected in human serum, platelets, and erythrocytes.[35,36,50] We presented several lines of experimental evidence to the brain origin of these MPs: (1) validation of BDMPs with a second set of neuronal and glial cell markers (supplemental Figure 5) and 90% to 98% of BDMPs stained positive for both sets of markers; (2) detection of MPs that are positive for GFAP, a much more specific marker for glial cells (Figure 1E),

and (3) identical flow cytometric profiles of BDMPs from TBI mice and those made from mouse brain (supplemental Figure 7). Interestingly, we did not detect NSE in mouse platelet microparticles (Figure 2B), suggesting that NSE in platelets may not be microparticle bound.

In reciprocal experiments, uninjured mice injected with BDMPs underwent a rapid and dose-dependent transition from a hypercoagulable state to a consumptive coagulopathy (Figure 3), as demonstrated by (1) a transition from mildly shortened to significantly prolonged clotting time, (2) a progressive reduction (depletion) of plasma fibrinogen with increasing dosing of BDMPs, and (3) widespread fibrin deposition in the vasculature. The observation that mice subjected to FPI developed a clearly defined hypercoagulable state, whereas coagulopathy rapidly occurred in mice injected with a similar number of BDMPs proceeded with a mild hypercoagulable state (Figure 1 vs 3), suggests that the speed of BDMP release into the circulation is critical for the development of coagulopathy. BDMPs were released over time from a traumatically injured brain but injected as a bolus (<5 minutes) into an uninjured mouse.

The procoagulant activity of BDMPs requires PS and TF on the surface of these microparticles because it was (1) detected in both PS-dependent and TF-dependent coagulation assays (Figure 2), (2) dose-dependently blocked by the PS-binding protein, lactadherin (Figure 2), and (3) greater than a comparable number of platelet microparticles that did not have a detectable level of TF (supplemental Figure 4). BDMP-facilitated thrombin generation had a delayed onset and smaller AUC compared with soluble human TF (Figure 2; Table 1). The distinct kinetics may result from (1) cooperativity between TF and PS coexpressed on BDMPs compared with soluble TF and PS added separately, (2) structural and functional differences between membrane-bound and soluble TF, and/or (3) species differences between BDMP-bound mouse TF and soluble human TF.

Another critical observation is that BDMPs were detected (albeit at a very low level) in mice exposed to sham surgery (Figure 1), likely due to minor injury associated with the surgery. The finding suggests that brain cells are highly sensitive to microvesiculation. This residual level of BDMPs had a minimal influence on coagulation in the
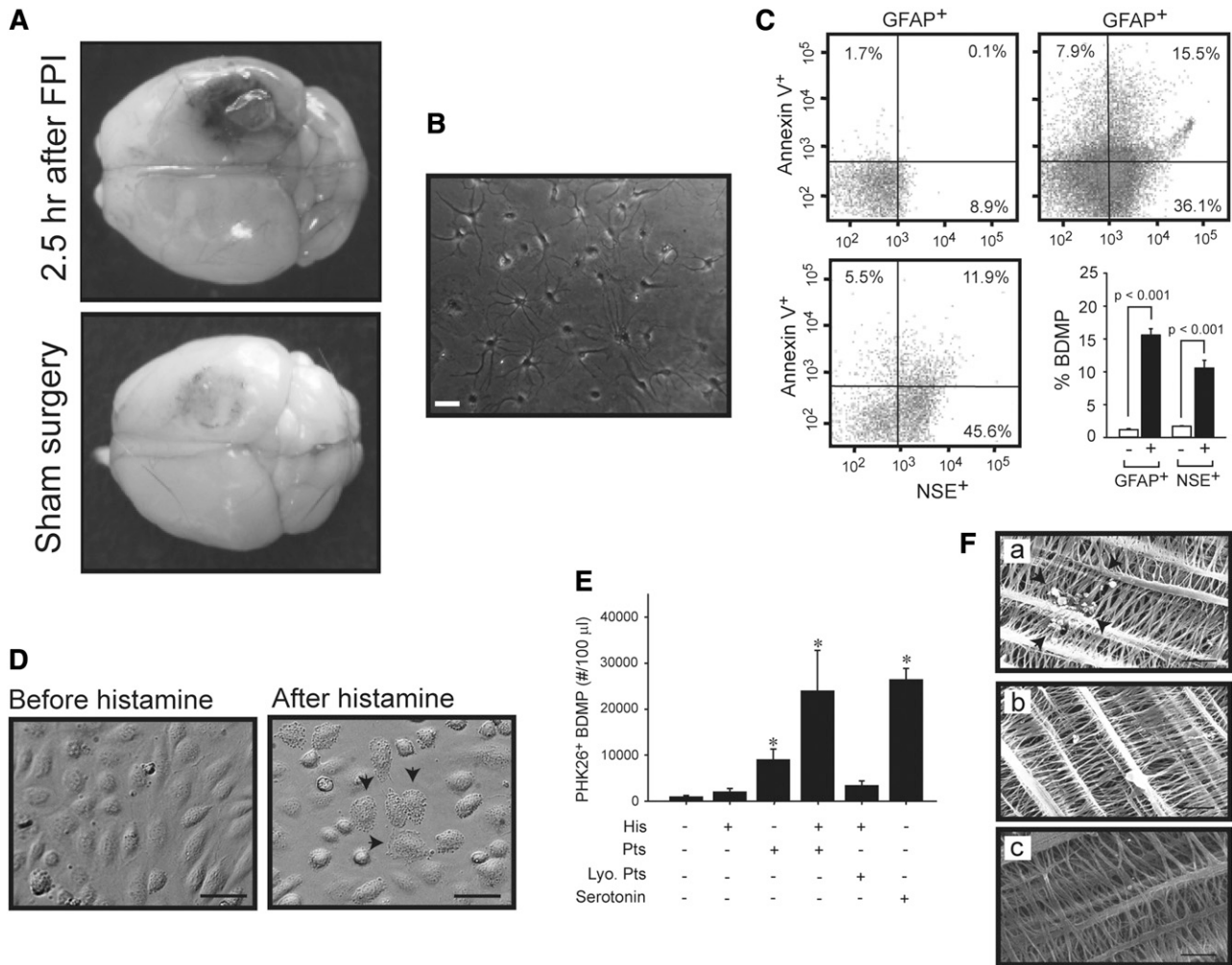
Figure 4. Production and transmigration of BDMPs. (A) Evans blue leaked from the vasculature of a mouse subjected to FPI, but significantly less from the one with sham surgery (representatives of 3 pairs of mice). (B) A representative image of hippocampal cells that were cultured for 7 days. (C) Cultured hippocampal cells were stimulated with 50 μM of the calcium ionophore A23187. The media collected (upper left) before and (upper right and lower left) after stimulation were analyzed for BDMPs by flow cytometry (n = 6, paired t test, $P < .001$). (D) HUVECs grown to confluence (left) become retracted and granulated (arrows) after being stimulated with 25 μM histamine (right; bar = 20 μm). (E) PKH26-labeled BDMPs detected in the bottom chamber by flow cytometry 3 hours after BDMPs were incubated with resting and histamine-activated (His) HUVECs in the presence and absence of 3×10^5/μL human live (Pts) or lyophilized (Lyo. Pts) platelets (n = 6/group, 1-way ANOVA, *$P < .005$ vs baseline). Serotonin (5 μM) also promotes microparticle transmigration in the absence of live platelets. (F) SEM images showing BDMPs (arrowhead) on the opposite side of the membrane from histamine-activated HUVECs that were incubated with BDMPs in the (a) presence and (b) absence of live platelets or (c) resting HUVECs incubated with BDMPs (bar = 5 μm).

acute stage of injury (Figure 1), but its long-term impacts, especially after repeated exposures, remain to be determined.

Second, we demonstrated that BDMPs activate platelets (Figure 5). Platelets may facilitate the transmigration of BDMPs through a disrupted endothelial barrier (Figure 4) by serving as a carrier or by promoting local inflammation at a site of vascular injury. The former is unlikely because the membrane pores used in the culture matrix of the transwell were 0.4 μm in diameter, substantially smaller than activated platelets (5-7 μm), and lyophilized platelets failed to support the transmigration (Figure 4E). In the latter case, BDMP-activated platelets release proinflammatory mediators that can induce or propagate local inflammation. One such mediator may be serotonin, as it has been previously reported to increase vascular permeability.[51] This inflammatory activity may explain why live, but not lyophilized, platelets promoted BDMP transmigration through unstimulated endothelial cells. Surprisingly, BDMPs did not directly induce platelet aggregation or enhance its induction by collagen, potentially due to the steric hindrance of BDMPs that prevents platelet-to-platelet contacts.

Third, we demonstrated the ability of lactadherin to block PS-dependent procoagulant activity (Figure 2E), raising 2 important perspectives. The first is that PS scavengers and PS-neutralizing molecules, such as lactadherin and annexin V, may reduce TBI-associated coagulopathy and BDMP-induced platelet activation. Annexin V has been reported to inhibit arterial thrombosis in a rabbit model of carotid artery injury.[52] The second is that an intrinsic or acquired deficiency in a PS-dependent clearance of microparticles may predispose an individual to TBI-associated consumptive coagulopathy. The molecules involved in the clearance and/or neutralization of PS$^+$ microparticles (and apoptotic cells) may thus have predictive and therapeutic values for coagulopathy associated with TBI and other pathologies.

In summary, we show that a traumatically injured brain releases procoagulant BDMPs into the circulation to promote intravascular coagulation and activate platelets. Our results call for clinical studies to detect BDMPs in the systemic circulation of patients with TBI and to investigate their contributions to the development of
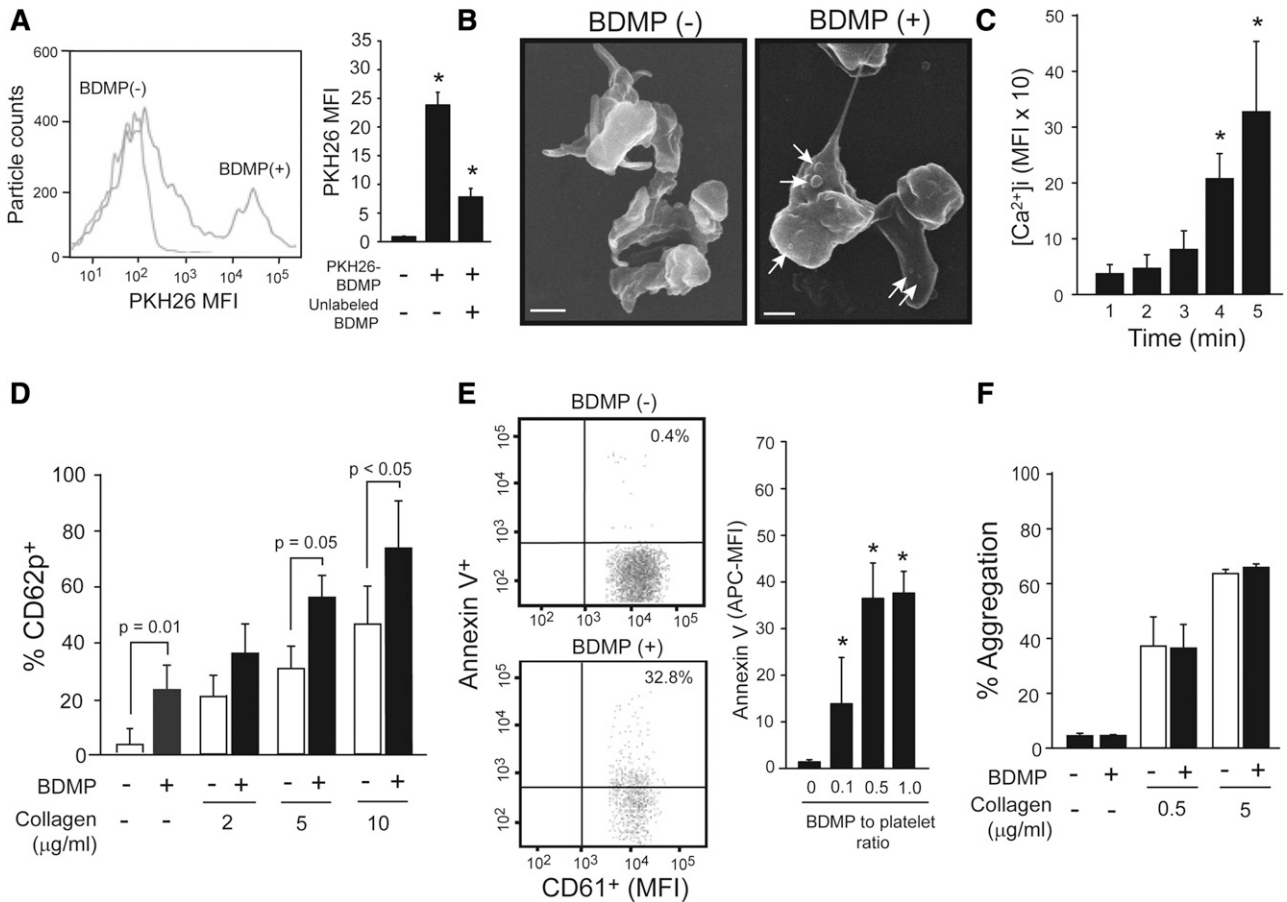
Figure 5. Effect of BDMPs on platelets. (A) Human platelets incubated with PKH26-labeled BDMPs and a CD61 antibody (10 minutes at 37°C) were gated on CD61 positivity and analyzed for PKH26 fluorescence by flow cytometry (1-way ANOVA, n = 12, *P < .01 compared with baseline). (B) Scanning electron microscopic images of platelets immobilized onto fibrinogen and incubated with either (left) PBS (bar = 1 μm) or (right) BDMPs (bar = 1 μm). (C) Calcium influx in platelets incubated with 25 000/μL BDMPs for the indicated times (n = 6, repeated-measures ANOVA, *P < .001, the values are after background subtraction). (D) CD62p expression was measured on platelets incubated with 25 000/μL BDMPs for 30 minutes at 37°C in the presence and absence of type I collagen (n = 6, paired t test). (E) Annexin V binding to platelets (CD61+) treated with BDMPs was measured by flow cytometry (n = 6, 1-way ANOVA, *P < .001 compared with baseline). (F) Human platelets were monitored for aggregation in an optical aggregometer after 25 000/μL BDMPs were added to 100 μL PRP with and without collagen (n = 6, paired t test).

coagulopathy and clinical outcomes. If validated in clinical studies, BDMPs in the circulation may serve as a predictive marker of TBI-associated coagulopathy and a therapeutic target for its prevention and treatment. Blood cells have been the focus on linking microparticles to the development of coagulation and inflammatory pathologies, but cancer cell-derived microparticles have increasingly been recognized for a role in the development of cancer-associated thrombosis.[53] Our results further suggest that microparticles from injured tissues/organs contribute to trauma-associated coagulopathy.

Authorship

Contribution: Y.T. and Y.Z. designed and performed experiments, provided data analysis, and wrote the manuscript; B.S. and M.W. designed and performed experiments and wrote the manuscript; H.Y., J.Y., Z.Z., and X.W. designed and performed experiments; B.A.K. designed experiments and wrote the manuscript; P.T. generated lactadherin, provided data analysis, and wrote the manuscript; and M.L., J.Z., and J.-f.D. developed hypotheses, designed experiments, analyzed data, and wrote the manuscript.

Conflict-of-interest disclosure: The authors declare no competing financial interests.

Correspondence: Jing-fei Dong, Puget Sound Blood Center Research Institute, 1551 Eastlake Ave East, Seattle, WA 98102; e-mail: jfdong@psbc.org; Jianning Zhang, Tianjin Neurological Institute, Department of Neurosurgery, General Hospital, Tianjin Medical University, Tianjin, 300052 China; e-mail: jianningzhang@hotmail.com; or Min Li, Institute of Pathology, School of Basic Medical Sciences, Lanzhou University, Lanzhou, 730000 China; e-mail: limin@lzu.edu.cn.

References

1. Niles SE, McLaughlin DF, Perkins JG, et al. Increased mortality associated with the early coagulopathy of trauma in combat casualties. *J Trauma.* 2008;64(6):1459-1463, discussion 1463-1465.

2. Mitra B, Cameron PA, Mori A, Fitzgerald M. Acute coagulopathy and early deaths post major trauma. *Injury.* 2012;43(1):22-25.

3. Wafaisade A, Wutzler S, Lefering R, et al; Trauma Registry of DGU. Drivers of acute coagulopathy after severe trauma: a multivariate analysis of 1987 patients. *Emerg Med J.* 2010;27(12): 934-939.

4. Maani CV, DeSocio PA, Holcomb JB. Coagulopathy in trauma patients: what are the main influence factors? *Curr Opin Anaesthesiol.* 2009;22(2):255-260.

5. Cohen MJ, Call M, Nelson M, et al. Critical role of activated protein C in early coagulopathy and later organ failure, infection and death in trauma patients. *Ann Surg.* 2012;255(2):379-385.

6. Cohen MJ, Kutcher M, Redick B, et al. Clinical and mechanistic drivers of acute traumatic coagulopathy. *J.Trauma Acute. Care Surg.* 2013; 75(1 Supp 1):S40-S47.

7. Talving P, Benfield R, Hadjizacharia P, Inaba K, Chan LS, Demetriades D. Coagulopathy in severe traumatic brain injury: a prospective study. *J Trauma.* 2009;66(1):55-61, discussion 61-62.

8. Hulka F, Mullins RJ, Frank EH. Blunt brain injury activates the coagulation process. *Arch Surg.* 1996;131(9):923-927, discussion 927-928.

9. Stein SC, Smith DH. Coagulopathy in traumatic brain injury. *Neurocrit Care.* 2004;1(4):479-488.

10. Harhangi BS, Kompanje EJ, Leebeek FW, Maas AI. Coagulation disorders after traumatic brain injury. *Acta Neurochir (Wien).* 2008;150(2): 165-175, discussion 175.

11. Lee TH, Hampton DA, Diggs BS, et al. Traumatic brain injury is not associated with coagulopathy out of proportion to injury in other body regions. *J Trauma Acute Care Surg.* 2014;77(1):67-72.

12. de Oliveira Manoel AL, Neto AC, Veigas PV, Rizoli S. Traumatic brain injury associated coagulopathy [published online ahead of print July 23, 2014]. *Neurocrit Care.*

13. Lentz BR. Exposure of platelet membrane phosphatidylserine regulates blood coagulation. *Prog Lipid Res.* 2003;42(5):423-438.

14. Kunzelmann-Marche C, Satta N, Toti F, et al. The influence exerted by a restricted phospholipid microenvironment on the expression of tissue factor activity at the cell plasma membrane surface. *Thromb Haemost.* 2000;83(2):282-289.

15. Phillis JW, Horrocks LA, Farooqui AA. Cyclooxygenases, lipoxygenases, and epoxygenases in CNS: their role and involvement in neurological disorders. *Brain Res Brain Res Rev.* 2006;52(2):201-243.

16. Zwaal RF, Comfurius P, van Deenen LL. Membrane asymmetry and blood coagulation. *Nature.* 1977;268(5618):358-360.

17. Fleck RA, Rao LV, Rapaport SI, Varki N. Localization of human tissue factor antigen by immunostaining with monospecific, polyclonal anti-human tissue factor antibody. *Thromb Res.* 1990;59(2):421-437.

18. Drake TA, Morrissey JH, Edgington TS. Selective cellular expression of tissue factor in human tissues. Implications for disorders of hemostasis and thrombosis. *Am J Pathol.* 1989;134(5): 1087-1097.

19. del Zoppo GJ, Yu JQ, Copeland BR, Thomas WS, Schneiderman J, Morrissey JH. Tissue factor localization in non-human primate cerebral tissue. *Thromb Haemost.* 1992;68(6):642-647.

20. Zillmann A, Luther T, Müller I, et al. Platelet-associated tissue factor contributes to the collagen-triggered activation of blood coagulation. *Biochem Biophys Res Commun.* 2001;281(2): 603-609.

21. Camera M, Frigerio M, Toschi V, et al. Platelet activation induces cell-surface immunoreactive tissue factor expression, which is modulated differently by antiplatelet drugs. *Arterioscler Thromb Vasc Biol.* 2003;23(9):1690-1696.

22. Alkhamis TM, Beissinger RL, Chediak JR. Artificial surface effect on red blood cells and platelets in laminar shear flow. *Blood.* 1990;75(7): 1568-1575.

23. Owens AP III, Mackman N. Microparticles in hemostasis and thrombosis. *Circ Res.* 2011; 108(10):1284-1297.

24. Davizon P, Munday AD, López JA. Tissue factor, lipid rafts, and microparticles. *Semin Thromb Hemost.* 2010;36(8):857-864.

25. Biró E, Akkerman JW, Hoek FJ, et al. The phospholipid composition and cholesterol content of platelet-derived microparticles: a comparison with platelet membrane fractions. *J Thromb Haemost.* 2005;3(12):2754-2763.

26. Krishnaswamy S, Field KA, Edgington TS, Morrissey JH, Mann KG. Role of the membrane surface in the activation of human coagulation factor X. *J Biol Chem.* 1992;267(36): 26110-26120.

27. Del Conde I, Shrimpton CN, Thiagarajan P, López JA. Tissue-factor-bearing microvesicles arise from lipid rafts and fuse with activated platelets to initiate coagulation. *Blood.* 2005;106(5): 1604-1611.

28. Nekludov M, Mobarrez F, Gryth D, Bellander BM, Wallen H. Formation of microparticles in the injured brain of patients with severe isolated traumatic brain injury. *J Neurotrauma.* 2014; 31(23):1927-1933.

29. Morel N, Morel O, Petit L, et al. Generation of procoagulant microparticles in cerebrospinal fluid and peripheral blood after traumatic brain injury. *J Trauma.* 2008;64(3):698-704.

30. Bianco F, Pravettoni E, Colombo A, et al. Astrocyte-derived ATP induces vesicle shedding and IL-1 beta release from microglia. *J Immunol.* 2005;174(11):7268-7277.

31. Ferrari D, Chiozzi P, Falzoni S, et al. ATP-mediated cytotoxicity in microglial cells. *Neuropharmacology.* 1997;36(9):1295-1301.

32. Duan S, Neary JT. P2X(7) receptors: properties and relevance to CNS function. *Glia.* 2006;54(7): 738-746.

33. Huang XT, Zhang YQ, Li SJ, et al. Intracerebroventricular transplantation of ex vivo expanded endothelial colony-forming cells restores blood-brain barrier integrity and promotes angiogenesis of mice with traumatic brain injury. *J Neurotrauma.* 2013;30(24): 2080-2088.

34. Shah MD, Bergeron AL, Dong JF, López JA. Flow cytometric measurement of microparticles: pitfalls and protocol modifications. *Platelets.* 2008;19(5): 365-372.

35. Marangos PJ, Campbell IC, Schmechel DE, Murphy DL, Goodwin FK. Blood platelets contain a neuron-specific enolase subunit. *J Neurochem.* 1980;34(5):1254-1258.

36. Day IN, Thompson RJ. Levels of immunoreactive aldolase C, creatine kinase-BB, neuronal and non-neuronal enolase, and 14-3-3 protein in circulating human blood cells. *Clin Chim Acta.* 1984;136(2-3):219-228.

37. Exner T, Joseph J, Low J, Connor D, Ma D. A new activated factor X-based clotting method with improved specificity for procoagulant phospholipid. *Blood Coagul Fibrinolysis.* 2003; 14(8):773-779.

38. Tchaikovski SN, VAN Vlijmen BJ, Rosing J, Tans G. Development of a calibrated automated thrombography based thrombin generation test in mouse plasma. *J Thromb Haemost.* 2007; 5(10):2079-2086.

39. Wallace PK, Tario JD Jr, Fisher JL, Wallace SS, Ernstoff MS, Muirhead KA. Tracking antigen-driven responses by flow cytometry: monitoring proliferation by dye dilution. *Cytometry A.* 2008; 73(11):1019-1034.

40. Quintarelli G, Zito R, Cifonelli JA. On phosphotungstic acid staining. I. *J Histochem Cytochem.* 1971;19(11):641-647.

41. Yang M, Chen J, Su F, et al. Microvesicles secreted by macrophages shuttle invasion-potentiating microRNAs into breast cancer cells. *Mol Cancer.* 2011;10:117.

42. Zhang Y, Liu X, Liu L, et al. Contact- and agonist-regulated microvesiculation of human platelets. *Thromb Haemost.* 2013;110(2):331-339.

43. Boilard E, Nigrovic PA, Larabee K, et al. Platelets amplify inflammation in arthritis via collagen-dependent microparticle production. *Science.* 2010;327(5965):580-583.

44. Ui-Tei K, Sato S, Miyake T, Miyata Y. Induction of apoptosis in a Drosophila neuronal cell line by calcium ionophore. *Neurosci Lett.* 1996;203(3): 191-194.

45. Majno G, Shea SM, Leventhal M. Endothelial contraction induced by histamine-type mediators: an electron microscopic study. *J Cell Biol.* 1969; 42(3):647-672.

46. Bottaro D, Shepro D, Peterson S, Hechtman HB. Serotonin, norepinephrine, and histamine mediation of endothelial cell barrier function in vitro. *J Cell Physiol.* 1986;128(2):189-194.

47. McNicol A, Israels SJ. Platelet dense granules: structure, function and implications for haemostasis. *Thromb Res.* 1999;95(1):1-18.

48. Dale GL, Friese P, Batar P, et al. Stimulated platelets use serotonin to enhance their retention of procoagulant proteins on the cell surface. *Nature.* 2002;415(6868):175-179.

49. Michel CC, Kendall S. Differing effects of histamine and serotonin on microvascular permeability in anaesthetized rats. *J Physiol.* 1997;501(Pt 3):657-662.

50. Paus E, Risberg T. Establishment and evaluation of a radioimmunoassay for neuron-specific enolase. A marker for small cell lung cancer. *Tumour Biol.* 1989;10(1):23-30.

51. Cloutier N, Paré A, Farndale RW, et al. Platelets can enhance vascular permeability. *Blood.* 2012; 120(6):1334-1343.

52. Thiagarajan P, Benedict CR. Inhibition of arterial thrombosis by recombinant annexin V in a rabbit carotid artery injury model. *Circulation.* 1997; 96(7):2339-2347.

53. Geddings JE, Mackman N. Tumor-derived tissue factor-positive microparticles and venous thrombosis in cancer patients. *Blood.* 2013; 122(11):1873-1880.